

# Examination of Bending Stress Superposition Effect on Martensite Transformation in Austenitic Stainless Steel 304

Elizabeth M. Mamros<sup>1</sup> , Lenard A. Polec<sup>2</sup>, Fabian Maaβ<sup>2</sup>, Till Clausmeyer<sup>2</sup>, A. Erman Tekkaya<sup>2</sup>, Jinjin Ha<sup>1</sup>, and Brad L. Kinsey<sup>1</sup>

**Abstract.** Uniaxial tension is a universal material characterization experiment. However, studies have shown that increased formability can be achieved with simultaneous bending and unbending of the material. This so-called continuous bending under tension process is an example of bending stress superposition to a uniaxial tension process. In this research, experiments are conducted on stainless steel 304 to investigate the effects of bending stress superposition on the austenite to martensite phase transformation. Two vortex tubes are mounted to the carriage of the machine and used to decrease the temperature in a localized region of the specimen to evaluate two temperature conditions. The *in-situ* strain and temperature fields are captured using 3D digital image correlation and infrared cameras. The deformation induced  $\alpha'$ -martensite volume fraction is measured at regular intervals along the deformed gauge length using a Feritscope. The number of cycles that the rollers traverse the gauge length, corresponding to the strain level, is also varied to create five conditions. The deformed specimens revealed heterogeneous martensite transformation along the gauge length due to the non-uniform temperature fields observed for each test condition. Decreasing the temperature and increasing the number of cycles led to the highest amount of phase transformation for this bending-tension superposed process. These results provide insight on how stress superposition can be applied to vary the phase transformation in more complex manufacturing processes, such as incremental forming, which combines bending, tension, and shear deformation.

**Keywords:** Martensite Transformation · Stainless Steel · Stress Superposition

## 1 Introduction

Incremental forming is a rapid prototyping process that can be used to manufacture customized sheet metal parts without requiring specialized tooling. In incremental forming, a tool, typically hemispherical, traverses a piece of clamped sheet metal following a layer-by-layer toolpath to form the desired geometry. The conventional process is known

<sup>&</sup>lt;sup>1</sup> Mechanical Engineering, University of New Hampshire, Durham, NH 03824, USA jinjin.ha@unh.edu

Institute of Forming Technology and Lightweight Components, TU Dortmund University, Dortmund. Germany

as single point incremental forming (SPIF) and results in increased material formability compared to stamping and deep drawing [1]. Three dominant forming mechanisms are observed during incremental forming: bending, tension, and shear [2], i.e., stress superposition. Stress superposition is defined as the incorporation of additional stresses into a primary forming operation during a single process step [3]. This innately stress-superposed process can be manipulated to affect the properties of the formed part [4], but complex modeling efforts are required to inform manufacturing decisions, e.g., process parameter selection.

To assist with modeling incremental forming, a similar, simpler manufacturing process, known as continuous bending under tension (CBT), can be investigated. The CBT process is more complex than uniaxial tension because bending, via rollers, is superposed to a uniaxial process but less complex than incremental forming, due to the absence of shear deformation. A numerical model of the CBT process was introduced by Hadoush et al. [5] to better understand the effects of cycling in sheet metal forming, specifically in relation to incremental forming and deformation beyond the forming limit curve. The deformation mechanisms in the CBT process have been likened to those of SPIF, including the bending depth to the wall angle and the roller speed of the carriage to the feed rate and step size. A CBT machine designed with an additional roller, which is subjected to a constant compression force, to superpose compression has been used to investigate the deformation mechanisms in double-sided incremental forming (DSIF) [6].

Several variations of CBT machines exist, including one at the University of New Hampshire (UNH) [7]. Previous studies have shown that the CBT process increases elongation to failure, i.e., the formability of the material, compared to uniaxial tension and decreases the required forming load. This is consistent with two of the three main objectives of using the stress superposition strategy, which are increased formability [8], reduced forming loads, and enabling customization [9], which will be demonstrated in this work through the manipulation of phase transformation. CBT experiments have been conducted for aluminum [10], magnesium [11], and dual phase steels [12] using the UNH machine to validate various material models used in finite element analyses.

Austenitic stainless steels undergo an irreversible strain-induced phase transformation from  $\gamma$ -austenite (face-centered cubic, FCC) to  $\alpha'$ -martensite (body-centered cubic, BCC). Alternatively, the phase transformation can occur from  $\gamma$ -austenite to  $\epsilon$ -martensite (hexagonal close packed, HCP) to  $\alpha'$ -martensite. This phase transformation is a function of several parameters including temperature [13], strain level [14], strain rate [15], strain path [16], stress state [17], crystallographic texture [18], stacking fault energy [19], and chemical composition [4]. Related to these parameters, certain grades of stainless steel (SS) transform at different rates when subjected to the same temperature and loading conditions, e.g., SS316L transforms significantly less than SS304 and SS301LN [20]. This variance dependent upon the material and a combination of parameters during experiments makes it difficult for martensitic transformation kinetics models to be transferable between materials and processes without modification.

As one example, a model proposed by Olson and Cohen in 1975 [14] has been adapted several times to include additional parameters in order to attempt to fit other materials. Their model, based on data from Angel [21], predicts the martensitic transformation as a function of equivalent plastic strain and temperature. In 1992, Stringfellow et al.

incorporated stress triaxiality into Olson and Cohen's model [22] to compare with the experimental results presented by Young [23]. Several years later, Tomita and Iwamoto amended the previous version of the model to include the effect of strain rate [24]. In 2011, Beese and Mohr expanded the model to incorporate the Lode angle parameter as another means to define the stress state in addition to the stress triaxiality [17]. The following year, Beese and Mohr proposed an anisotropic version of their model to account for the differences in phase transformation observed previously for rolling direction and transverse direction SS301LN uniaxial tension tests [25]. For additively manufactured SS304L, Wang and Beese proposed a stress state dependent model that also accounts for the crystallographic texture and chemical composition of the material [18]. Future numerical analyses of the CBT process will include martensitic transformation kinetics modeling for the chosen material.

In this work, continuous bending under tension experiments are conducted on stainless steel 304, to investigate the effects of bending stress superposition on the austenite to martensite phase transformation. Two temperature conditions and five strain levels, i.e., varied numbers of cycles, are investigated to determine the effects of localized cooling and strain level on the phase transformation of this material. A Feritscope is used to measure the  $\alpha'$ -martensite volume fraction along the gauge length, and the results are validated by electron backscatter diffraction (EBSD) analyses of select samples. In future work, x-ray diffraction analyses will be conducted to determine the effect of temperature and strain level variation on the residual stress development due to phase transformation. Finite element analyses will also be performed and validated by experimental results.

## 2 Material Characterization

#### 2.1 Material

Uniaxial tension experiments were conducted using the geometry described in the ASTM E8 standard and the procedure detailed in [26] to characterize 1.2 mm thick sheets of SS304, which are fully austenite in the undeformed condition (i.e., zero  $\alpha'$ -martensite volume fraction). The chemical composition provided by the manufacturer is shown in Table 1. The resulting true stress-strain curves from specimens oriented along the rolling direction (RD) is shown in Fig. 1. Note that starting at ~0.20 true strain, the strain hardening behavior of SS304 increases, which is an indication of the  $\alpha'$ -martensite phase transformation occurring.

	С	Si	Mn	P	S	Cr	Mo	Ni	N	Cu	Fe
SS304	0.07	1.00	2.00	0.045	0.030	16.71	_	10.12	_	_	Bal

Table 1. Chemical composition provided by manufacturer for SS304.

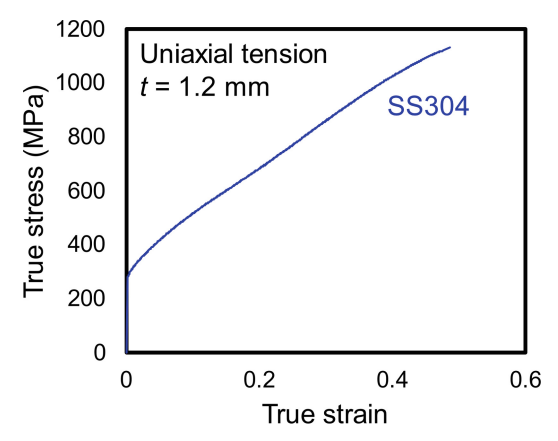


Fig. 1. True stress-strain curve for SS304 from uniaxial tension experiment oriented along the RD.

## 2.2 Specimen Preparation

The ASTM E8 geometry with an extended gauge length of 200 mm was used for the CBT experiments as shown in Fig. 2. The specimens were cut from the sheets along the RD by laser. The top surfaces of the specimens were prepared with layers of white paint, a black speckle pattern, and matte clear paint for detection in the digital image correlation post-processing software.



Fig. 2. Specimen geometry for CBT experiments.

## 3 Experiments

## 3.1 Experimental Setup

A custom CBT machine at UNH [7, 27] was used for experiments and is shown in Fig. 3. The CBT specimen was clamped in the grips, and the center roller of the three stationary roller system was displaced downward to create the bending condition. During the experiments, the cylinder was displaced to apply axial tension to one end of the specimen while the opposite side of the specimen remained fixed. The entire carriage assembly was driven by a ball screw and motor, which caused the specimen to traverse

through the stationary rollers over the gauge length of the specimen while superposing bending to the tensile process. To capture the strain and temperature *in-situ*, a stereo (3D) digital image correlation (DIC) system (Correlated Solutions Inc.) with two 2.3 megapixel cameras (FLIR Grasshopper2) and 17 mm lenses (Schneider) was coupled with an SC-645 infrared camera (FLIR). The three cameras were fixtured to the carriage, using aluminum extrusion and 3D-printed camera mounts as shown in Fig. 3, to allow the cameras to remain focused on the same area of interest throughout the experiment. Subset, step, and filter sizes of 4 pixels, 9 pixels, and 5 were used for all analyses (VIC-3D, Correlated Solutions Inc.).

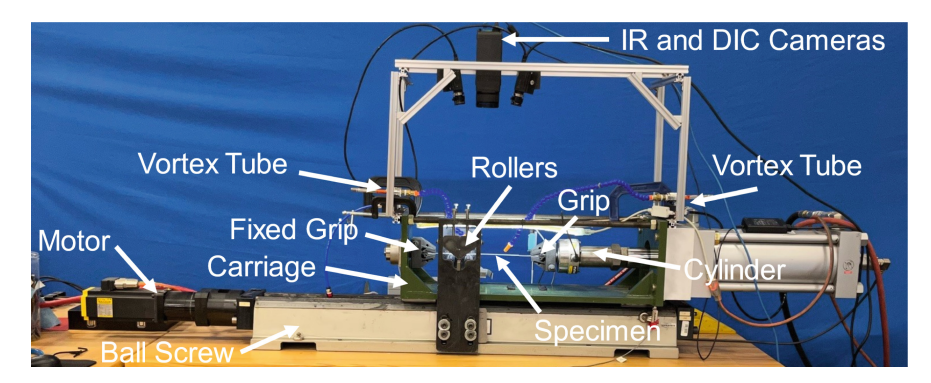


Fig. 3. CBT machine at the University of New Hampshire.

Based on previous experiments using this machine, the speed of the carriage, which is the so-called roller speed, was set to 66 mm/s, and the pulling speed, which is the speed of the cylinder, was set to 1.3 mm/s. The bending depth, which is the ratio of the bend depth from the rollers to the material thickness, was 2 for all experiments.

## 3.2 Temperature Control

To locally control the temperature, two vortex tubes (Vortec) were mounted to the carriage with 3D-printed fixtures, and the attached nozzles were aimed at two locations along the gauge length in the DIC area of interest (Fig. 4). Note that the cooling effect was extremely localized, and two controlled zones were created in the gauge area. The amount of hot air exhausted from the vortex tubes was adjusted to create two temperature conditions, low and high temperatures.

#### 3.3 Phase Transformation Measurements

The  $\gamma$ -austenite to  $\alpha'$ -martensite phase transformation in stainless steel was measured using an FMP30C Feritscope (Fischer Technology) on the unpainted, bottom surface of the specimens. The fixed end of the specimen was designated as the reference location, and measurements were taken every 12.7 mm along the gauge length after 10 cycles. The strain and temperature data were extracted at the same locations.

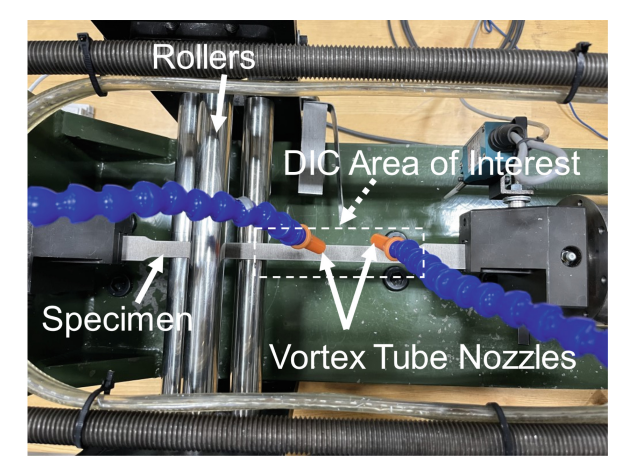


Fig. 4. Close-up of experimental setup from cameras' perspective.

To validate the  $\alpha'$ -martensite measurements from the Feritscope, electron backscatter diffraction (EBSD) analyses were performed on select samples extracted near P3 after 10 cycles (Table 2). A Tescan Lyra3 GMU focused ion beam scanning electron microscope equipped with an Edax EBSD detector was used for these analyses. The following parameters were selected: magnification: 750x; beam intensity: 19.1; acceleration voltage: 10 kV; sample tilt:  $70^\circ$ ; binning:  $8\times 8$ ; and step size:  $0.7~\mu m$ .

**Table 2.** Comparison of Feritscope and EBSD  $\alpha'$ -martensite measurements near P3.

Material	Temperature Condition	$\alpha'$ -Martensite Volume Fraction	
		Feritscope	EBSD
SS304	Low	0.89	0.82
	High	0.75	0.72

## 4 Results

#### 4.1 Strain

The true strain evolution along the pulling direction in the gauge length of a SS304 specimen deformed at the low temperature condition with different number of cycles is shown in Fig. 5. The strain field is relatively uniform over the gauge length throughout the forming process and reaches a true strain value of approximately 0.35 after 10 cycles.

## 4.2 Temperature

The evolution of the temperature in the gauge length with increasing deformation, i.e., number of cycles, is shown for a SS304 low temperature experiment in Fig. 6. The two

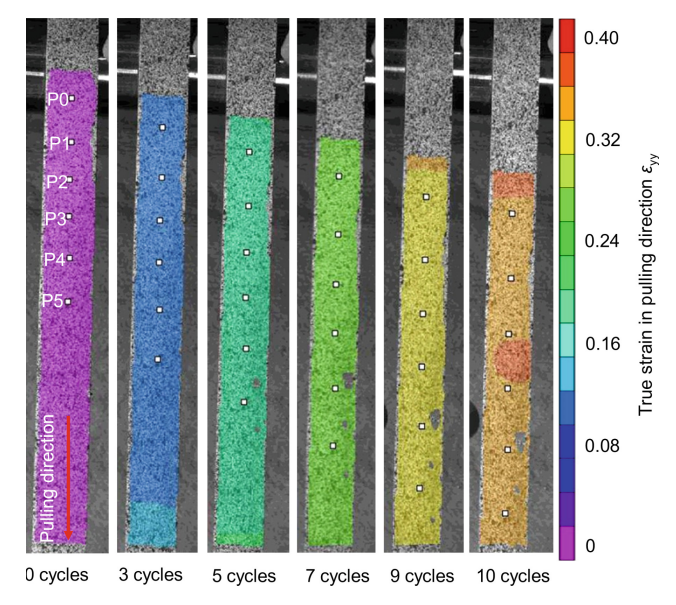


**Fig. 5.** Evolution of true strain in pulling direction ( $\varepsilon_{yy}$ ) recorded in gauge length of SS304 low temperature CBT specimen at 0 (undeformed), 3, 5, 7, 9, and 10 cycles.

controlled zones created by the vortex tubes are distinguishable by their reduced temperature compared to the rest of the area of interest. Note that the controlled zones appear to remain stationary, but, due to elongation, different regions of the gauge area passed through the controlled zones as the experiment progressed. Throughout the experiment shown in Fig. 6, the temperature in the center of the controlled zones increases  $\sim$ 4°. In the surrounding regions, the temperature increases  $\sim$ 11 °C since the cooling effect of the vortex tubes is lessened significantly at distances farther away from the nozzle. At the extreme captured by the thermal camera, i.e., near the bottom of Fig. 6, the temperature increases to nearly 30 °C due to the lack of temperature control and deformation-induced heating.

Comparing Figs. 5 and 6, it appears that the localized cooling did not cause significant inhomogeneity in the true strain in the pulling direction in the region of interest. However, the DIC images of each cycle were captured after the rollers had traversed the area of interest. Some localized effects on the strain may occur when the rollers pass through the controlled zones and superpose bending, but, unfortunately, these regions were obscured from the cameras' view.

#### 4.3 Martensitic Transformation

From Olson and Cohen [14], it is known that increased martensitic transformation occurs at decreased temperatures and increased strain levels. Both trends were observed for the  $\alpha'$ -martensite volume fraction of SS304 when comparing the low temperature and high temperature conditions at varying numbers of cycles as shown in Fig. 7. The average volume fraction over the area of interest for three specimens at each condition is plotted

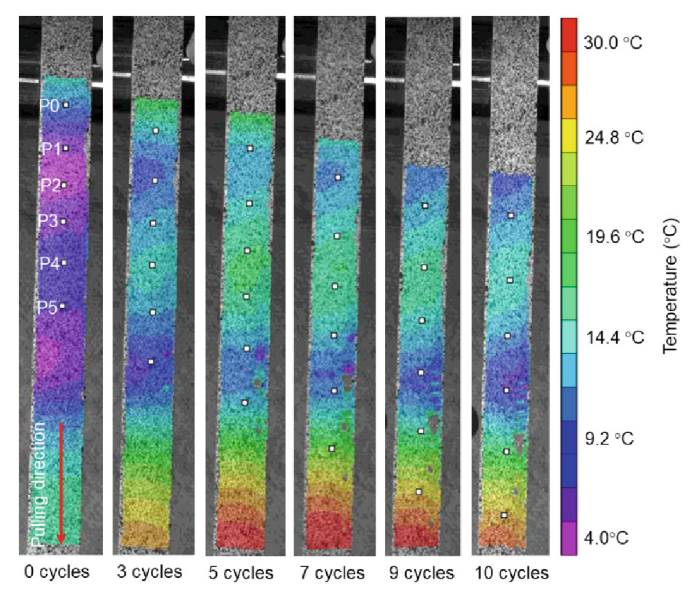


**Fig. 6.** Evolution of temperature recorded in gauge length of SS304 low temperature CBT specimen at 0 (undeformed), 3, 5, 7, 9, and 10 cycles.

with vertical error bars representing the maximum and minimum values from the three specimens' averages and horizontal error bars representing the true strain values recorded by the DIC after the designated number of cycles.

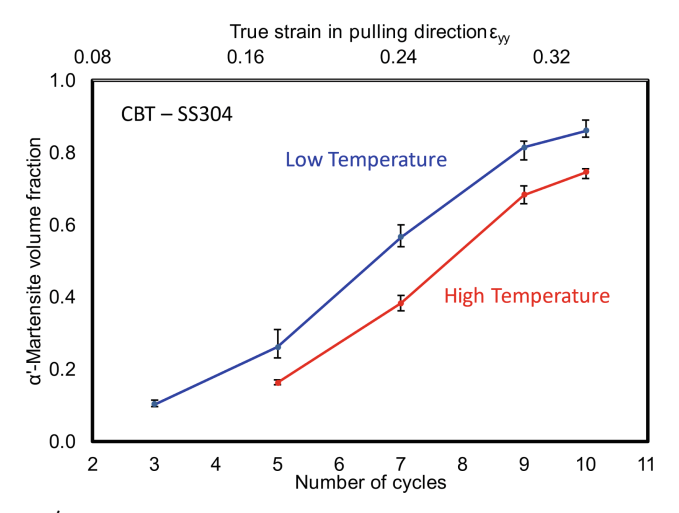
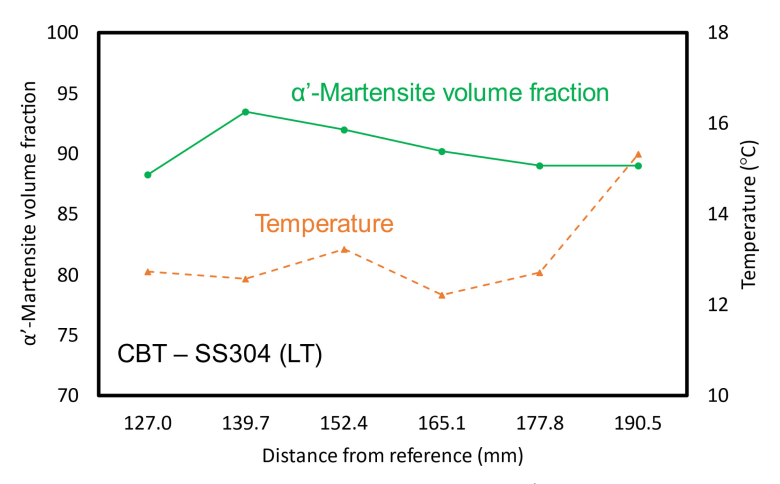


Fig. 7. Average  $\alpha'$ -martensite volume fraction in the area of interest of SS304 low temperature and high temperature CBT experiments with respect to true strain in pulling direction and number of cycles.

The  $\alpha'$ -martensite volume fraction and average temperature at the analysis points in the area of interest vary slightly along the gauge length of the specimen. An example from a SS304 low temperature, 10 cycles experiment is shown in Fig. 8. The  $\alpha'$ -martensite volume fraction varies ~0.05, and the temperature varies ~3°. Again, the analysis points in the area of interest moved through the cooling regions created by the vortex tubes as the specimen was elongated, so different locations with respect to the reference were exposed to varying amounts of cooling throughout the experiment. Note that the accuracy of the Feritscope is not guaranteed above 97.1% volume fraction [28].



**Fig. 8.** SS304 low temperature, 10 cycle CBT experiment:  $\alpha'$ -martensite volume fraction and average temperature measurements in the area of interest.

## 5 Conclusions

SS304 specimens were subjected to continuous bending under tension experiments conducted at high and low temperature conditions, which were created using vortex tubes. The  $\alpha'$ -martensitic phase transformation resulting from the stress superposition of bending onto a tension process was evaluated using a Feritscope. Five strain levels, corresponding to 3, 5, 7, 9, and 10 cycles, were investigated.

Increased strain levels and decreased temperature conditions led to increased phase transformation. The strain in the pulling direction remained relatively homogeneous throughout the experiments, while the temperature varied due to the presence of two controlled zones created by the vortex tubes and deformation-induced heating. The variation in material properties along the gauge length, e.g., volume fraction, supports that stress superposition can be used in manufacturing processes to achieve functionally graded materials.

**Acknowledgements.** Support for the New Hampshire Center for Multiscale Modeling and Manufacturing of Biomaterials (NH BioMade) project is provided by the US National Science Foundation (NSF) EPSCoR award (#1757371). This research is also supported by the German Academic

Exchange Service (DAAD) Research Internships in Science and Engineering (RISE) Worldwide. Special thanks to Dirk Hoffmann from IUL for his assistance with specimen preparation. The SEM/FIB used is managed by the University Instrumentation Center (UIC) at UNH and was purchased with funds awarded from the US National Science Foundation (NSF) (MRI Grant 1337897) with additional funds from UNH.

## References

- 1. Martins, P.A.F., Bay, N., Skjoedt, M., Silva, M.B.: Theory of single point incremental forming. CIRP Ann. 57, 247–252 (2008). https://doi.org/10.1016/j.cirp.2008.03.047
- Allwood, J.M., Shouler, D.R., Tekkaya, A.E.: The increased forming limits of incremental sheet forming processes. Key Eng. Mater. 344, 621–628 (2007). https://doi.org/10.4028/www. scientific.net/KEM.344.621
- 3. Tekkaya, A.E., Groche, P., Kinsey, B.L., Wang, Z.G.: Plasticity and future opportunities of stress superposition in metal forming. CIRP Ann. (under revision) (2023)
- Feng, Z., Mamros, E.M., Ha, J., et al.: Modeling of plasticity-induced martensitic transformation to achieve hierarchical, heterogeneous, and tailored microstructures in stainless steels. CIRP J. Manuf. Sci. Technol. 33, 389–397 (2021). https://doi.org/10.1016/j.cirpj.2021.04.006
- Hadoush, A., Van den Boogaard, T., Huetink, J.: Stable incremental deformation of a strip to high strain. Int. J. Mach. Tool Manuf. 344(615), 620 (2007). https://doi.org/10.4028/www. scientific.net/KEM.344.615
- Peng, W., Ou, H.: Deformation mechanisms and fracture in tension under cyclic bending plus compression, single point and double-sided incremental sheet forming processes. Int. J. Mach. Tools 184, 103980 (2023). https://doi.org/10.1016/j.ijmachtools.2022.103980
- Roemer, T.J., Kinsey, B.L., Korkolis, Y.P.: Design of a continuous-bending-under-tension machine and initial experiments on Al-6022-T4. Am. Soc. Mech. Eng. Digit. Collect. (2015). https://doi.org/10.1115/MSEC2015-9440
- Barrett, T., Kinsey, B.L., Knezevic, M., Korkolis, Y.P.: Numerical and experimental investigation of formability enhancement during continuous-bending-under-tension (CBT) of AA6022-T4. Procedia Eng. 207, 1940–1945 (2017). https://doi.org/10.1016/j.proeng.2017. 10.965
- Maaß, F., Hahn, M., Tekkaya, A.E.: Adjusting residual stresses by flexible stress superposition in incremental sheet metal forming. Arch. Appl. Mech. 91(8), 3489–3499 (2021). https://doi. org/10.1007/s00419-021-01929-x
- Zecevic, M., Knezevic, M.: Origins of improved elongation to fracture in cyclic bending under tension of AA6022-T4 sheets as revealed using crystal plasticity modeling. Mech. Mater. 177, 104546 (2023). https://doi.org/10.1016/j.mechmat.2022.104546
- Matukhno, N., Kljestan, N., Vogel, S.C., Knezevic, M.: Cyclic bending under tension of alloy AZ31 sheets: influence on elongation-to-fracture and strength. Mater. Sci. Eng. A 857, 144127 (2022). https://doi.org/10.1016/j.msea.2022.144127
- 12. Poulin, C.M., Korkolis, Y.P., Kinsey, B.L., Knezevic, M.: Over five-times improved elongation-to-fracture of dual-phase 1180 steel by continuous-bending-under-tension. Mater. Des. **161**, 95–105 (2019). https://doi.org/10.1016/j.matdes.2018.11.022
- Mamros, E.M., Bram Kuijer, M., Davarpanah, M.A., Baker, I., Kinsey, B.L.: The effect of temperature on the strain-induced austenite to martensite transformation in SS 316L during uniaxial tension. In: Daehn, G., Cao, J., Kinsey, B., Tekkaya, E., Vivek, A., Yoshida, Y. (eds.) Forming the Future. TMMMS, pp. 1853–1862. Springer, Cham (2021). https://doi.org/10. 1007/978-3-030-75381-8\_155

- Olson, G., Cohen, M.: Kinetics of strain-induced martensitic nucleation. Metall. Trans. A 6, 791–795 (1975). https://doi.org/10.1007/BF02672301
- 15. Talonen, J., Nenonen, P., Pape, G., Hänninen, H.: Effect of strain rate on the strain-induced  $\gamma \rightarrow \alpha'$ -martensite transformation and mechanical properties of austenitic stainless steels. Metall. Mater. Trans. A **36**, 421–432 (2005). https://doi.org/10.1007/s11661-005-0313-y
- Darzi, S., Adams, M.D., Roth, J.T., et al.: Manipulating martensite transformation of SS304L during double-sided incremental forming by varying temperature and deformation path. CIRP Ann. Manuf. Technol. (2023)
- Beese, A.M., Mohr, D.: Effect of stress triaxiality and Lode angle on the kinetics of straininduced austenite-to-martensite transformation. Acta Mater. 59, 2589–2600 (2011). https:// doi.org/10.1016/j.actamat.2010.12.040
- Wang, Z., Beese, A.M.: Stress state-dependent mechanics of additively manufactured 304L stainless steel: Part 1 characterization and modeling of the effect of stress state and texture on microstructural evolution. Mater. Sci. Eng. A 743, 811–823 (2019). https://doi.org/10.1016/j.msea.2018.11.094
- Neding, B., Tian, Y., Ko, J.Y.P., Hedström, P.: Correlating temperature-dependent stacking fault energy and in-situ bulk deformation behavior for a metastable austenitic stainless steel. Mater. Sci. Eng. A 832, 142403 (2022). https://doi.org/10.1016/j.msea.2021.142403
- Katajarinne, T., Kivivuori, S.: Strain induced martensite in incremental forming formation, effect and control. MSF 773–774, 119–129 (2013). https://doi.org/10.4028/www.scientific.net/MSF.773-774.119
- Angel, T.: Formation of martensite in austenitic stainless steels, effect of deformation, temperature and composition. J. Iron Steel Inst. 177, 165–174 (1954)
- Stringfellow, R.G., Parks, D.M., Olson, G.B.: A constitutive model for transformation plasticity accompanying strain-induced martensitic transformations in metastable austenitic steels.
  Acta Metall. Mater. 40, 1703–1716 (1992). https://doi.org/10.1016/0956-7151(92)90114-T
- Young, C.-C.: Transformation toughening in phosphocarbide-strengthened austenitic steels.
  Massachusetts Institute of Technology (1988)
- Tomita, Y., Iwamoto, T.: Constitutive modeling of trip steel and its application to the improvement of mechanical properties. Int. J. Mech. Sci. 37, 1295–1305 (1995). https://doi.org/10.1016/0020-7403(95)00039-Z
- Beese, A.M., Mohr, D.: Anisotropic plasticity model coupled with Lode angle dependent strain-induced transformation kinetics law. J. Mech. Phys. Solids 60, 1922–1940 (2012). https://doi.org/10.1016/j.jmps.2012.06.009
- Mamros, E.M., Mayer, S.M., Banerjee, D.K., et al.: Plastic anisotropy evolution of SS316L and modeling for novel cruciform specimen. Int. J. Mech. Sci. 234 (2022). https://doi.org/10.1016/j.ijmecsci.2022.107663
- 27. Roemer, T.: Experimental apparatus for continuous-bending-under-tension and experiments on A6022-T4. Master's theses and capstones (2016)
- Talonen, J., Aspegren, P., Hänninen, H.: Comparison of different methods for measuring strain induced martensite content in austenitic steels. Mater. Sci. Technol. 20, 1506–1512 (2004). https://doi.org/10.1179/026708304X4367